agriculture

Article

Computational Model for the Dynamic Characterisation of a Trunk Shaker

Pedro Sanchez-Cachinero, Rafael Luque-Mohedano and Rafael R. Sola-Guirado *

Department of Mechanics, Campus de Rabanales, University of Cordoba, 14014 Cordoba, Spain
* Correspondence: ir2sogur@uco.es

Abstract: The development of trunk shaker machines over the years has been based on test-error methods in field. Mathematical or computational models have been studied with great simplifications. This paper presents a method for modelling the dynamic behaviour of a trunk shaker with a test bench. Two mass configurations were used on the test bench as well as two different vibration frequencies on the trunk shaker. Acceleration values were recorded at different points of the system. The binomial shaker-post was computationally modelled, and its dynamic response was analysed based on a modal and transient study with a series of proposed simplifications. The results of the simulations were compared with experimentally recorded acceleration values. In both cases, a linear response to mass and frequency variation was observed in the acceleration that the shaker performed. There was a high correlation in the effective accelerations (error < 4%) between experimental and computational studies measured in the trunk shaker. However, there were higher errors when the post was used in the test in the post structure points. The greatest uncertainty in the model may lie in the assumption of contact between the attachment pad and the post, but if this is not carried out, it makes convergence in the computational calculations very difficult. The method has proved its worth in determining the dynamic behaviour of these machines.

Keywords: vibration; mechanical harvesting; virtual simulation; dynamic response; CAD FEM

check for updates

Citation: Sanchez-Cachinero, P.; Luque-Mohedano, R.; Sola-Guirado, R.R. Computational Model for the Dynamic Characterisation of a Trunk Shaker. *Agriculture* **2022**, *12*, 2158. https://doi.org/10.3390/agriculture12122158

Academic Editor: Daniela Farinelli

Received: 16 November 2022
Accepted: 13 December 2022
Published: 15 December 2022

1. Introduction

Harvesting is usually the costliest operation for most fruit trees. Mechanisation of this operation can improve profit margins by using machinery adapted to the plantation and trees trained to the machines. Intensive plantation models use canopy shaker systems for harvesting [1–3]. However, many plantations do not have these modern arrangements and are mechanically harvested by other kinds of machines. Trunk shakers are a very useful technology for harvesting different fruits such as olives, nuts, and citrus fruits [4]. The most-used systems today, due to their simplicity, are orbital trunk shakers which have an eccentric mass rotating at high speed inside a clamp with the ability to grip the tree trunks and apply a forced vibration. This vibration must be efficiently transmitted along the tree structure to the bearing branches.

These machines have evolved considerably over several decades with the major premise of maximizing fruit removal while minimising tree damage. It is estimated that at least 85% harvesting efficiency is required for trunk shaker harvesting to be viable [5]. Field tests are often carried out on different trees in order to optimise trunk shaker technology with a very high empirical component. Over the years, machinery manufacturers have developed a multitude of trunk shaker models with different improvements that have advanced through field tests on a test-error premise. In order to continue advancing in the improvement of technology, it would be very useful to create a reliable and detailed computer model that would allow as many design modifications as desired to be made without the need for these costly field tests.

There are several parameters that are directly related to the vibration to be transmitted by the machine such as the vibration frequency, the amplitude of the movement, or the clamping system design (contact surface; type of clamping or clamping force) [6,7]. A multitude of parameters also play a role from the point of view of the tree, in general terms: mass and distribution, stiffness, and damping, which are quite different along the plant and between different trees [8–10]. This high variability leads to the difficulty of optimising the trunk shakers, as many trees with substantial differences are required, waiting for the harvesting time, and considering the possible damage that may happen. Therefore, a test bench could be a suitable solution to improve the machines or to predict the forces and displacements generated [11].

The main model used by researchers to characterise the behaviour of the trunk shaker are based on the dynamic equilibrium equation based on the mass, stiffness, damping, and force of the system [12]. Several authors have studied the tree behaviour with a forced vibration using mathematical equations based on trees properties [13,14]. Theorical studies have been also carried out with the binomial tree-trunk shaker, for example, to forecast the vibration power for optimal harvesting [15]. In recent years, different authors have developed computational models as a tool for predicting the dynamic behaviour of trees. The most-used model is the finite element method. El-Awady et al. simulates an olive-tree in three dimensions to analyse the behaviour of the tree structure versus the fruit arrangement found [16]. Other authors analyse the different vibration modes found in trees under different loading mode [17,18]. Wu et al. reconstructs a virtual tree and studies the dynamics of the model [19]. Centinkaya et al. characterises the dynamic response of a test bench to different configurations of the mass system of a kind of shaker using as tools a simulated environment to obtain the possible resonances in the system [20]. Hoshyarmanesh et al. proposes to analyse the behaviour of one virtual tree structure (without foliage) with a trunk shaker with critical simplifications [21]. Other authors seek to find the best configurations to produce the fruit detachment of different trees with experimental tests [22,23].

However, these works base their models on what happens in the vibration applied from the trunk to the branches and do not present methodologies for the characterisation of the machine as such. The wide range of the design possibilities and parameters of the shaker clamps lies in the possibility of generating different vibration patterns or different effects on the trees. For example, knowing the acceleration distribution in the different axes of the machine can influence harvesting efficiencies [24] and even its application in some axes can generate bark damage with irreversible damage to the plantation [25]. Modal analysis of the machines would determine the optimal working frequencies and vibration modes [26]. Therefore, obtaining a computational model that replicates the virtual dynamic behaviour of the machine can be a major improvement in the sector. However, the computational simulations can be too complex at present [27] and simplifications in the models are necessary so that the calculations can lead to adequate solutions [21]. The objective of this work is to propose and validate a methodology to characterise the dynamic behaviour of trunk shakers. The development of a computational model for the simulation of a trunk shaker working on a test bench is presented in order to maintain repeatability conditions in the tests. The results of the computational simulations will be contrasted with the experimental conditions on the test bench by analysing the effect produced by the frequency variation in the trunk shaker and the mass variation at the top of the post.

2. Materials and Methods

2.1. Trunk Shaker

The geometrical model of an experimental orbital trunk shaker (Figure 1) which has been manufactured using the usual manufacturing techniques of any machinery manufacturer (cutting of sheet metal and profiles, bending, welding, etc.). The trunk shaker has an eccentric mass of 60 kg whose centre of mass with respect to the point of rotation is 118 mm. This mass is driven by a vane motor (Veljan VM4D-128, Hyderabad, India). This motor is powered by the hydraulic flow provided by a 100 cm^3 variable displacement piston pump (Rexroth A10V100 EK, Lohr am Main, Germany) with a theoretical flow rate of 200 l min^{-1} at 2000 rpm. This pump is driven by the power take-off of a tractor (John Deere 6420, Moline, USA) at a working speed of 540 rpm where the tractor engine speed was set at 2200 rpm. This tractor has been mounted with a front structure that allows the tractor head to move towards and turn around the trunk of the trees. The shaker head is suspended at the end of this structure on silent-blocks and metal chains. The head has two hydraulic cylinders that move two mobile arms that pivot on joints located at the end of the head to open and close for gripping the trunk. These joints are adjustable to modify the parallelism of the pads in the opening and closing process but for this study they have been fixed in an extreme position (Figure 1). At the end of these movable arms rubber blocks are fitted which are deformed when the system closes with the tree to avoid damaging the tree bark.

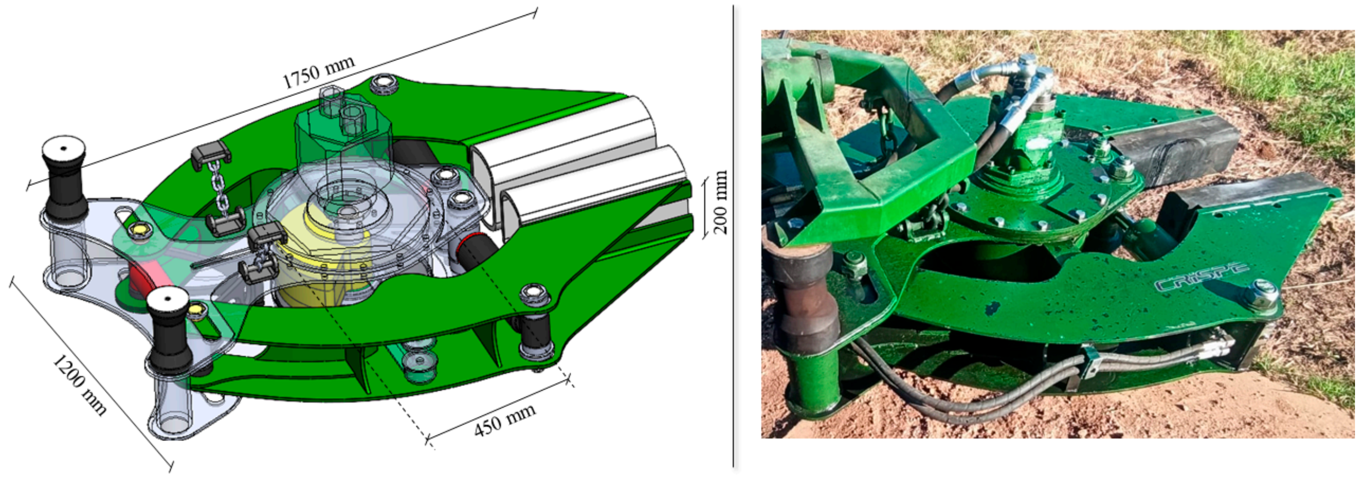

Figure 1. Trunk shaker designed (**left**) and fabricated and mounted on the tractor (**right**).

2.2. Test Bench

The geometric model of a test bench has been designed and manufactured with the aim of carrying out the necessary tests for the experimental and computational study (Figure 2). The aim is to simulate an artificial tree with the major differences that may exist, but seeking to achieve a structure that allows a multitude of tests to be carried out without modifying its mechanical properties as would be the case in real trees. The system consists of a hollow metal base of 1500 mm in diameter and 450 mm high, weighing 2020 kg. In the centre of the base, anchors have been placed to raise the support plate where the artificial trunk will be installed. In such a way that there is a hollow space that can be filled with any ballast, such as sand, and thus prevent the base of the structure from moving during vibration and at the same time it can be transported to different locations with a crane. A steel post 200 mm in diameter, 8 mm thick and 1500 mm high, weighing 56 kg is welded into the plate. This post could be modified by another one with a different section simulating a different mass of the trunk of the tree but in this work only this one has been used. At the top of the post a circular plate was welded to simulate the canopy of the tree with two 20 × 100 mm cross-section plates, 1500 mm long, arranged in a cross. Different masses can be superposed on this system to vary the mass conditions of the canopy, although in this work two configurations were used: a set of one cross (one mass of 46 kg) and a set of three crosses (three masses of 138 kg).

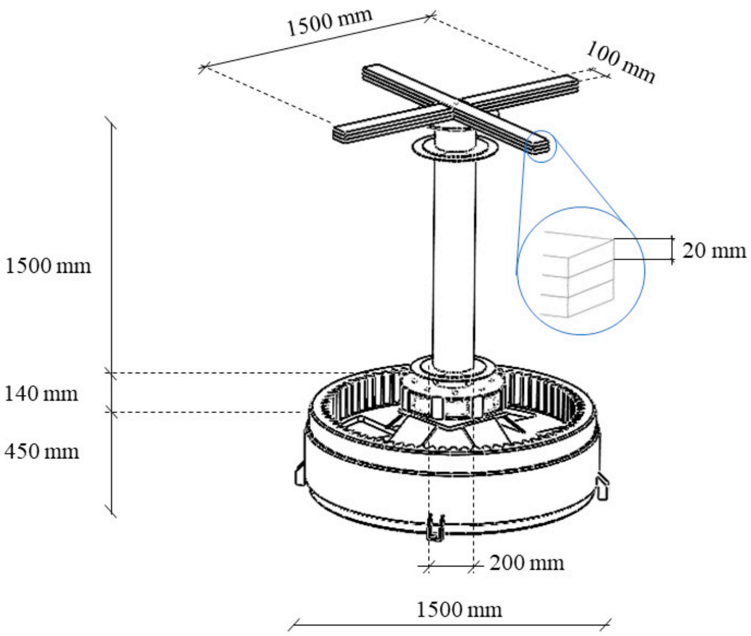

Figure 2. Test bench made together with the trunk shaker set up for the vibration test (**right**) and dimensions test bench (**left**).

2.3. Experimental Study with the Trunk Shaker and the Test Bench

Different tests have been carried out with the trunk shaker manufactured as shown below. In the first study, the vibration generated by the trunk shaker in a free state was characterised. To do this, it was suspended horizontally by pressing the pad to pad and vibration was applied by measuring the acceleration generated at the end of the arm close to the block. In a second study, the vibration generated on the test bench was characterised by placing it horizontally and perpendicular to the post at a height of 76 mm from the base, pressing pads centred on the post, giving a distance between the supports of 410 mm between the plates that grip the blocks (distance used in later studies 3.1).

With each of these two studies a 10 s vibration was carried out with a start-up ramp of 1 s until its permanent regime and a quick stop of 0.5 s. Four different configurations were studied by modifying the rotational speed of the vibration motor (different frequency) and modifying the mass of the test bench to be vibrated. The engine displacement was modified by placing rings that report 102 and 138 cubic centimetres with respective speeds of 1380 and 1080 rpm to modify the speed of rotation. With these configurations, vibrations with a frequency of 23 and 18 Hz, respectively, were measured in the workshop. One mass or three masses were welded to the top of the post, as described in Section 2.2, to modify the mass of the post. Each of these tests was carried out three times.

In each test, the accelerations generated in the assembly were recorded using three triaxial piezoelectric accelerometers (PCB Piezotronics 356A32, New York, NY, USA) connected to a dynamic signal analyser (OROS 36 Mobi-Pack, Meylan, France). The accelerometers were placed on the head of the shaker clamp; on the post in the grip height between the two pads and on the post of the top near the junction point with the cross-masses (Figure 3). After each repetition, the clamp was opened and closed to relieve internal stresses in the pads generated in the previous vibration maintaining parallelism and height between floor and the base of the test bench and the shaker. It was assumed that the oil temperature was similar and the tractor working rates were kept stable.

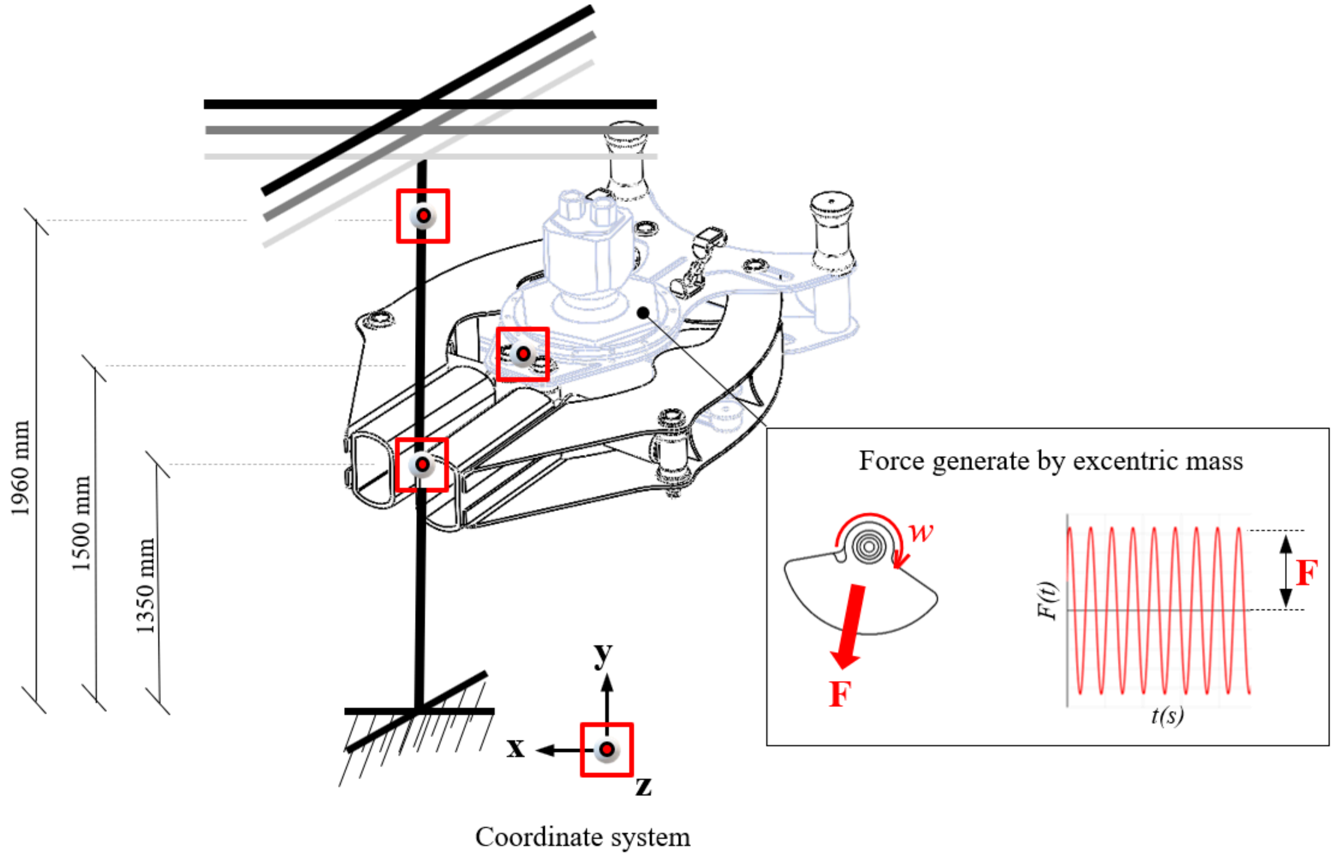

Figure 3. Position of the accelerometers on the test bench.

The following is the nomenclature used in each of the tests together with the respective study points.

- (C-f-F18): Configuration with trunk shaker vibrating free at a steady-state frequency of 18 Hz.
- (C-f-F23): Configuration with trunk shaker vibrating free at a steady-state frequency of 23 Hz.
- (C-p1m-F18): Configuration with 1 mass on the post with the trunk-shaker vibrating at a steady-state frequency of 18 Hz.
- (C-p3 m-F18): Configuration with 3 masses on the post and 18 Hz on the trunk shaker.
- (C-p1m-F23): Configuration with 1 mass on the post and 23 Hz on the trunk shaker.
- (C-p3m-F23): Configuration with 3 masses on the post and 23 Hz on the trunk shaker.

2.4. Computational Test

As many simulations were performed as the experimental tests with the same configurations. Once the calculations were completed three points were chosen in the geometry of the computational model that coincide with the points where the accelerometers were installed in the experimental test (Figure 3). At each point, the acceleration values as a function of time were obtained for each axis of the coordinate system. Of the 10 s of vibration set, 5 were analysed in which the vibration remained stable in a permanent regime. A fast Fourier transform (FFT) was used to determine the root mean square (RMS) acceleration of each accelerometer axis in the main frequency domain. The resultant acceleration was determined as the vector sum of each of the three axes. The transmissibility of the acceleration was calculated as the ratio (%) between two different points along the vibration path: Trunk shaker–Post in the grip; Trunk shaker–Top of the post; Post in the grip–Top of the post.

3. Preparations of the Computational Model

The model of the trunk shaker designed with the Solid-Works 2020 software (Waltham, MA, USA) was exported to the Ansys 19.2 software (Canonsburg, PA, USA) to compute its dynamic behaviour. All the tests carried out in Section 2.3 have been replicated by means of a series of virtual simulations for which it has been necessary to establish a methodology for the modelling and calculation described below:

3.1. Preparation of the Geometry of the Trunk Shaker Pads

The shaker pads deform when they press on the element to be vibrated in order to achieve a grip with the largest possible surface area that does not damage the trunk and prevents slippage. An 'Static Structural' analysis was carried out to obtain the characteristic geometry of this deformed pad. Firstly, the geometry of the trunk shaker was simplified in the CAD 'Computer Assistant Design' software 'Space Claim', leaving only the elements involved in the calculation. The structure or movable arms of the locking/opening and their pads, as well as the test bench to be used as mentioned above (Figure 4). Then, the material properties of the pads were adjusted by setting it as a hyperelastic material from its deformation constants. For this purpose, the Monney-Rivlin constants related to the hardness of the cue were used, which was experimentally determined as 65 shore, in shore scale A [28]. The forces necessary for the clamp to close were then applied to the model in such a way that the distance between the pads supports was the same as the distance determined experimentally in the tests. In this way, the pads are forced to deform while adapting to the post. The mesh obtained from the deformed dowel was exported in 'stl' format. This point cloud was edited again in the 'SpaceClaim' tool to create an isolated solid with the deformed pad. The geometry of the deformed pad (Figure 4 left) was replaced in the original CAD of the trunk shaker.

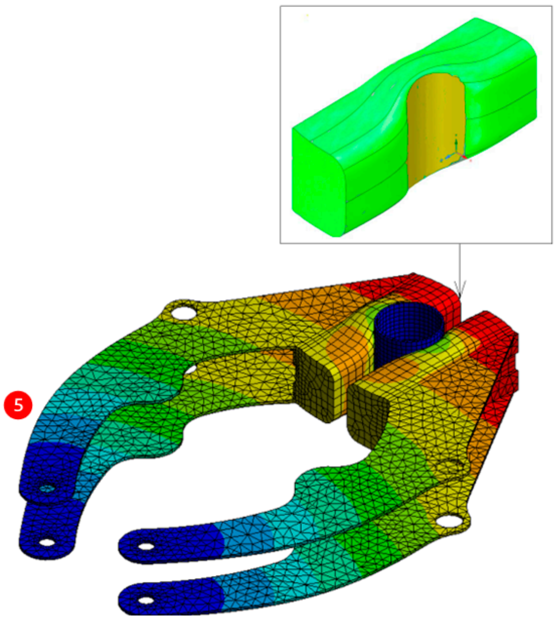

Components	Contact	Type
(1)	support	fixed
(2)	joint	revolute
(3)	contact	frictionless
(4)	joint	spring
(5)	Automatic mesh. Mixed between tetrahedon and hexahedron of second order. Quality set to 0.2	

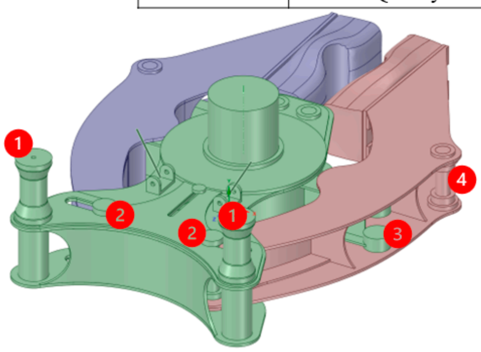

Figure 4. Geometry of the deformed pad (**left**) and geometry of the trunk shaker simplified for dynamic simulation (**right**).

3.2. Determination of the Variable Forces Generating Vibration

The load generated by the rotating eccentric mass was calculated in a 'Rigid Dynamics study'. The rotation of the trunk shaker mass was simulated around a support that simulates the behaviour of a bearing at the angular velocity that was established in the real tests. The force generated by the trunk shaker is a force of equal module with a constant change of direction. It is directly related to the weight of the mass, the eccentricity, and the square of angular velocity. The reactions in the bearing calculated with the tool were exported and used in a later step.

3.3. Preparation of the Geometry of the Trunk Shaker

The CAD model of the trunk shaker and the deformed pad was imported into the 'Space Claim' tool to perform a series of simplifications aimed at lightening the simulation (Figure 4 right):

- Holes, fasteners, roundings, and other geometries that do not affect the calculation were removed.
- All tolerances between components were removed and all components were made to match.
- Elements of complex geometry, such as the engine, were simplified while maintaining volumes and weights like the real ones.
- The components of the machine were grouped according to their relative mobility to each other obtaining the casing that houses the unbalance masses and the two arms that originate the blind and opening.
- Special elements such as chains which support the suspended trunk shaker are replaced by bar elements (link180) which are then configured in the next step to work only in traction.
- The hydraulic cylinders that perform the opening and closing of the clamp are replaced by 'spring' type elements so that they can be configured to generate a clamping tension if desired. However, in this work they were configured with a very high stiffness to resemble a fixed bar and maintain the position of the clamp closed in the vibration process.
- The eccentric mass was eliminated leaving only the shaft that supports it. In subsequent steps, a shaft density was defined to simulate the total mass of the system and further on it was configured to generate the loads exerted by the eccentric mass, calculated in step 3.2, applied on the shaft itself.

3.4. Dynamic System Analysis

A "Modal" study was carried out as the basis for a 'Transient structural'. With this configuration, the calculation time is significantly reduced by using the 'MSUP' modal superposition method incorporated in the Ansys tool. The mechanical properties of the materials of each element were defined in the 'Engineering data' section: The steel components are defined as 'Structural Steel' (default material) equivalent to the steel used in the fabrication (S355). The eccentric mass shaft was defined as the same steel but with the density modified to maintain the actual weight of the shaft-mass assembly. The elastomeric elements mainly rubbers (clamping support between the head and the structure of the tractor, as well as the cleats) were considered as an incompressible elastic material. It is assigned a Poisson's coefficient of 0.49. Young's modulus is obtained indirectly from its shore hardness [28]. This is a compromise solution since the rubbers are hyperelastic materials with non-linear behaviour which would need to be tested to obtain their hyperelasticity coefficients but doing it this way does not allow the 'MSUP' method to be used since it is only compatible with linear studies. The geometry of the complete trunk shaker was imported into the 'Geometry' study. The "Mechanical" tool was used to define the contacts and connections ('contact, joint') between the different components of the shaker, surfaces, joints, supports, etc. (Figure 5, right).

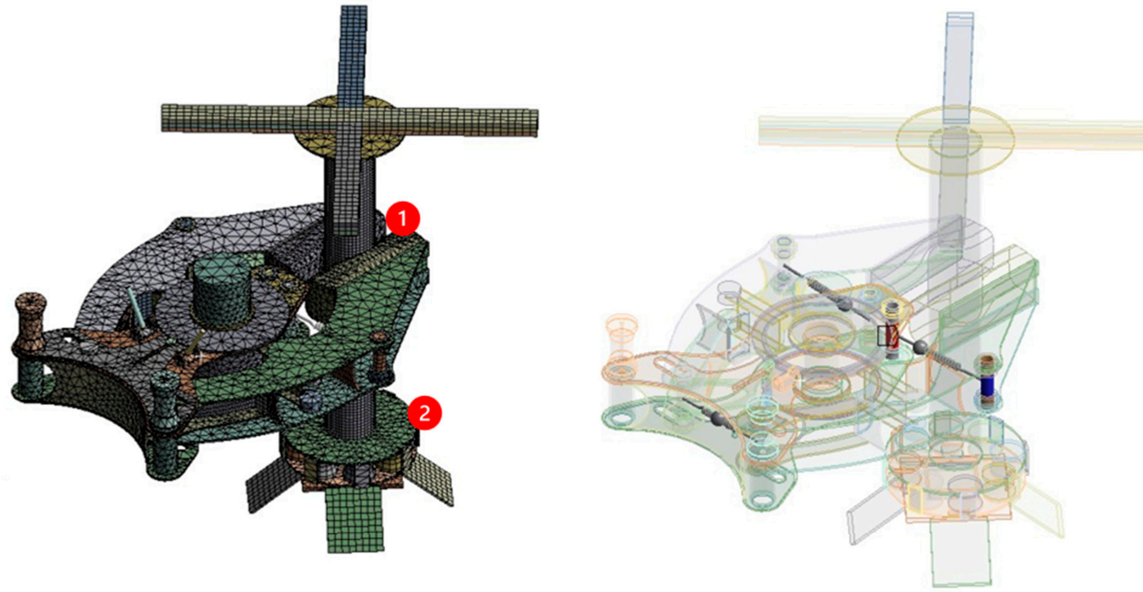

Components	Contact	Type
(1)	contact	bonded
(2)	support	fixed

Figure 5. Meshing (**left**) and 'Connections' (**right**) defined in the simplified model of the trunk shaker and test bench.

The main connections used were as follows. 'Joint fixed body to ground' between a fixed reference (points where the head is suspended) and the head housing, as well as the areas where the base of the trainer is attached. 'Revolute' and 'frictionless' type 'contact' joints at the scissor-type clamp joint between the frame and the clamps. 'Spring type joint' at the place of the opening and closing cylinders with a high 'longitudinal stiffness' constant of elasticity (10^7 N/mm) so that its behaviour resembles that of a steel bar with similar capacities to the cylinder in a fixed position.

The contact between the pads and post is configured as a 'bonded' type contact that does not allow relative displacements between the two solids. This last consideration generates uncertainty in the calculation, since there is a certain amount of sliding between the pads and the post that cannot be simulated in the type of study that has been carried out.

'Mesh' was defined for the whole assembly with all its default options. In specific areas where greater precision is required, a 'sizing' is applied to alter the mesh size as needed, as in the case of the joints, the chain, the pads and the post (Figure 5, left). The mesh applicated was a mix of hexahedron and tetrahedron of second order with a quality parameter of 0.2 and a medium smoothing.

4. Results

Table 1 shows the resulting accelerations generated by the trunk shaker in the experimental free test and its respective virtual simulation. The level of similarity in the resulting acceleration between the two tests was high, around 94% and 97% for frequencies of 18 Hz and 23 Hz, respectively, always considering the results of the experimental tests as the reference ones. The computational model reported slightly higher resultant acceleration values.

Table 1. Resultant accelerations (m s^{-2}) of trunk shaker free for both models.

	Computational Model	Test Bench
C-f-F18	115.49	109.01
C-f-F23	195.88	190.11

Figure 6 shows the resultant acceleration values in the frequency spectrum for the different study points measured (Figure 3) in the different trunk shaker and test bench configurations. The predominant frequencies of the computational model coincide with the experimental results, since the engine revolutions introduced as input in the computational model were the same as those used in the experimental tests. In the trunk shaker, the acceleration values had a high level of similarity with relative errors of less than 4% between the experimental test and the computational model, especially with 1 mass on the post. However, at the points post in the grip and top of the post, the percentage error increases between the measured and the simulation. The highest levels of variation between the computational model vs. experimental test were obtained at the point of contact between the trunk shaker and the top of the post. It can also be seen that the error is greater in the tests carried out at 18 Hz with variations between 50–80%, than in the tests carried out at 23 Hz where the errors decrease between 1–20%.

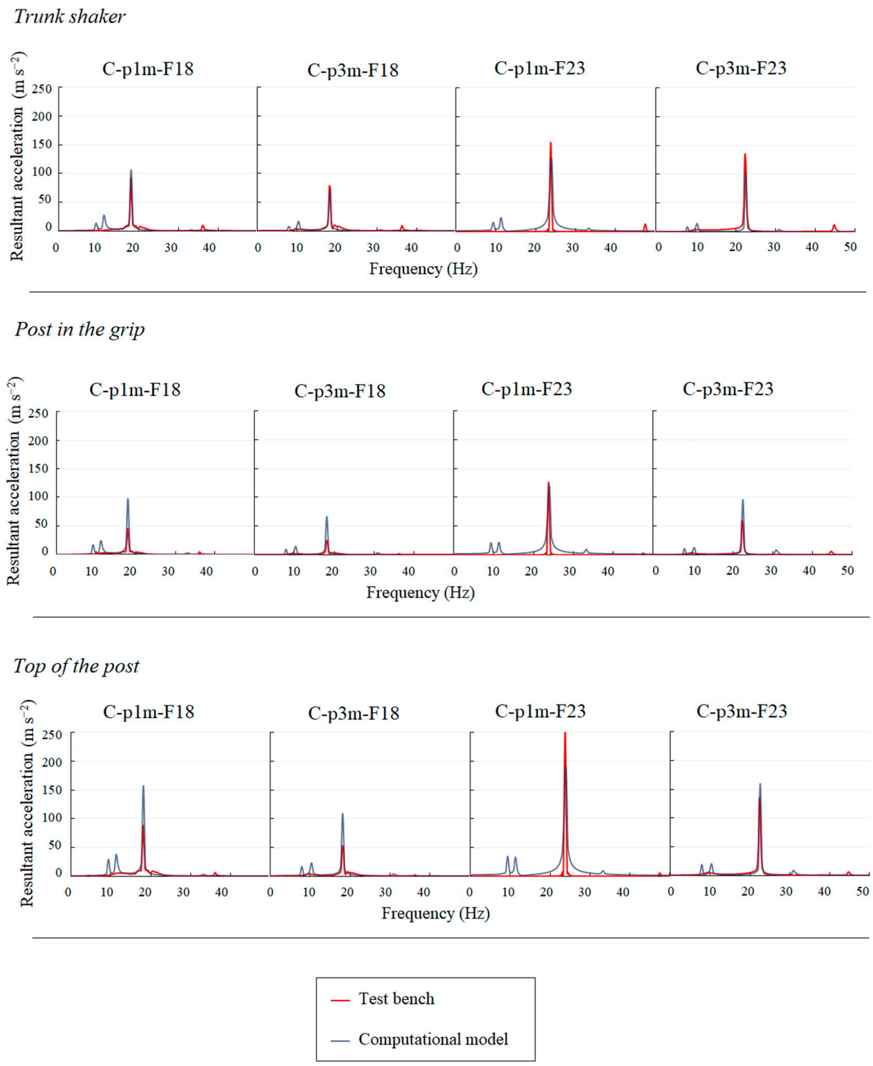

Figure 6. Vibration spectrum of the computational model and the experimental model recorded at the 3 study points.

Looking at how the frequency increases from 18 to 23 Hz (at the same post configuration with 1 mass or 3 masses) we can see that:

- In the free vibration, the trunk shaker shows a similar increase in both models, around 174%.
- The percentage increase in trunk shaker is around 130% being similar between measured and predicted by the computational model.
- In the post structure there is an increase in acceleration of around 210–270% in the experimental test, and 140–170% in the computational simulation, with similar increases between post in the grip and top of the post.

Looking at how increasing the mass on the test bench from 46 to 138 kg (at the same trunk shaker frequency configuration) we can see that:

- The resultant acceleration values decrease in all cases.
- In the trunk shaker the resultant acceleration drops to around 90% and 70% in the experimental and computational test, respectively, from 46 to 138 kg of post mass.
- At the points of the post structure, the resulting acceleration decreases by approximately 61% in the measurement and 65% in the simulation. This decrease is greater at higher frequencies in all cases. The percentages are similar for the post at the grip and the top of the post.

Figure 7 shows the vibration transmissibility along the trunk shaker-test bench. Experimental tests provided high repeatability in each configuration, with the standard deviation being lower than 0.5% (in terms of acceleration transmissibility) for 18 Hz frequency configurations and 4% for 23 Hz frequency configurations. A decrease in energy is observed from the trunk shaker to the post in the grip in both models and for all the proposed configurations. Between the post in the grip and top of the post an increase in acceleration is found in both models and in each of the configurations being almost double in the experimental case and ×1.6 in the computational model. Higher transmissivity values were obtained with increasing the frequency of the shaker, maintaining mass of the post; and lower values with increasing the mass of the post and maintaining the frequency of the shaker. The computational model responds in a less attenuated way to these variables, with C-p1m-F18 and C-p3m-F18 being the configurations that offer the greatest discrepancy with respect to the experimental tests.

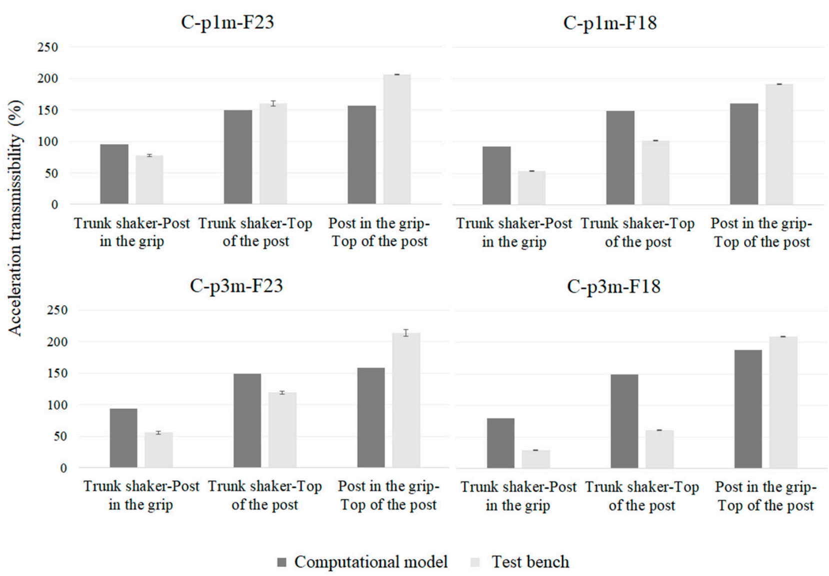

Figure 7. Acceleration transmissibility (%) between Trunk shaker–Post in the grip, Trunk shaker–Top of the post, and Post in the grip–Top of the post for the configuration considered.

Figure 8 shows the elliptical acceleration orbits recorded in both models at the top of the post. These comprise 5 s of steady vibration and lie in the xz plane of vibration (Figure 3). The computational model plotted trajectories very similar to those measured experimentally in terms of their order of magnitude and shape, although with differences that are reflected in the thickness of the generated orbit. The trajectories generated in the experimental model define a less equivoque path than the one recorded in the computational model. Compared to the experimental model, these distributions do not show any inclination of their principal axes against the coordinate axes. At the same frequency, increasing the mass of the post to be shaken results in a flatter acceleration orbit with less circularity. At the same mass, the *x*-axis of the acceleration increases with increasing frequency.

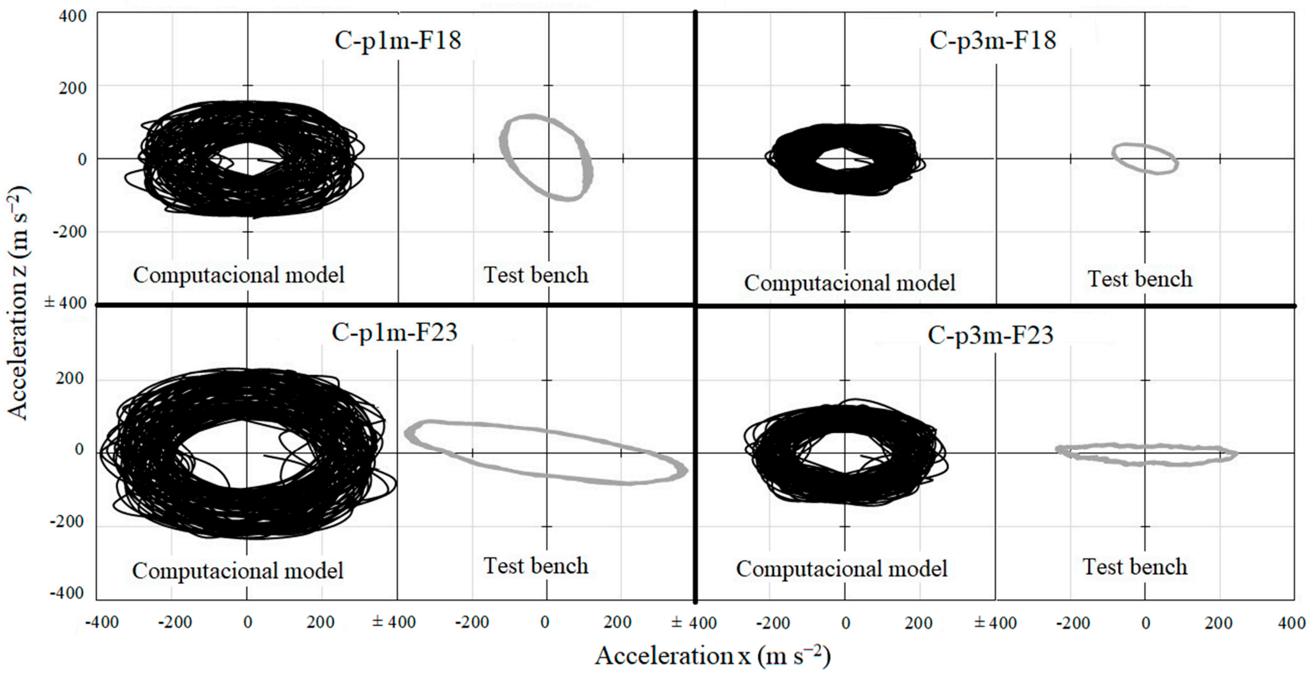

Figure 8. Orbits of accelerations recorded at Top of the post for the configurations considered.

The results obtained in modal analysis show the different modes of vibration found in the system. These may vary slightly from the real modes of vibration; however, it is possible to predict the behaviour in an approximate way. The first mode is found at 3.9 Hz where the model reproduces a movement along the *z*-axis (Figure 9), finding the maximum deformations at the high points of the test bench. The second mode of vibration is at 6.8 Hz causing a movement along the *x*-axis, (Figure 9). The maximum deformations were again found in the superior part of the model; however, they increased from 1.7 mm to 2.3 mm compared to the first vibration mode. The third mode of vibration is found at 10.8 Hz generating a torsional movement in the vibrator and finding the maximum deformations at the sides of the vibrator (2.8 mm maximum) (Figure 9).

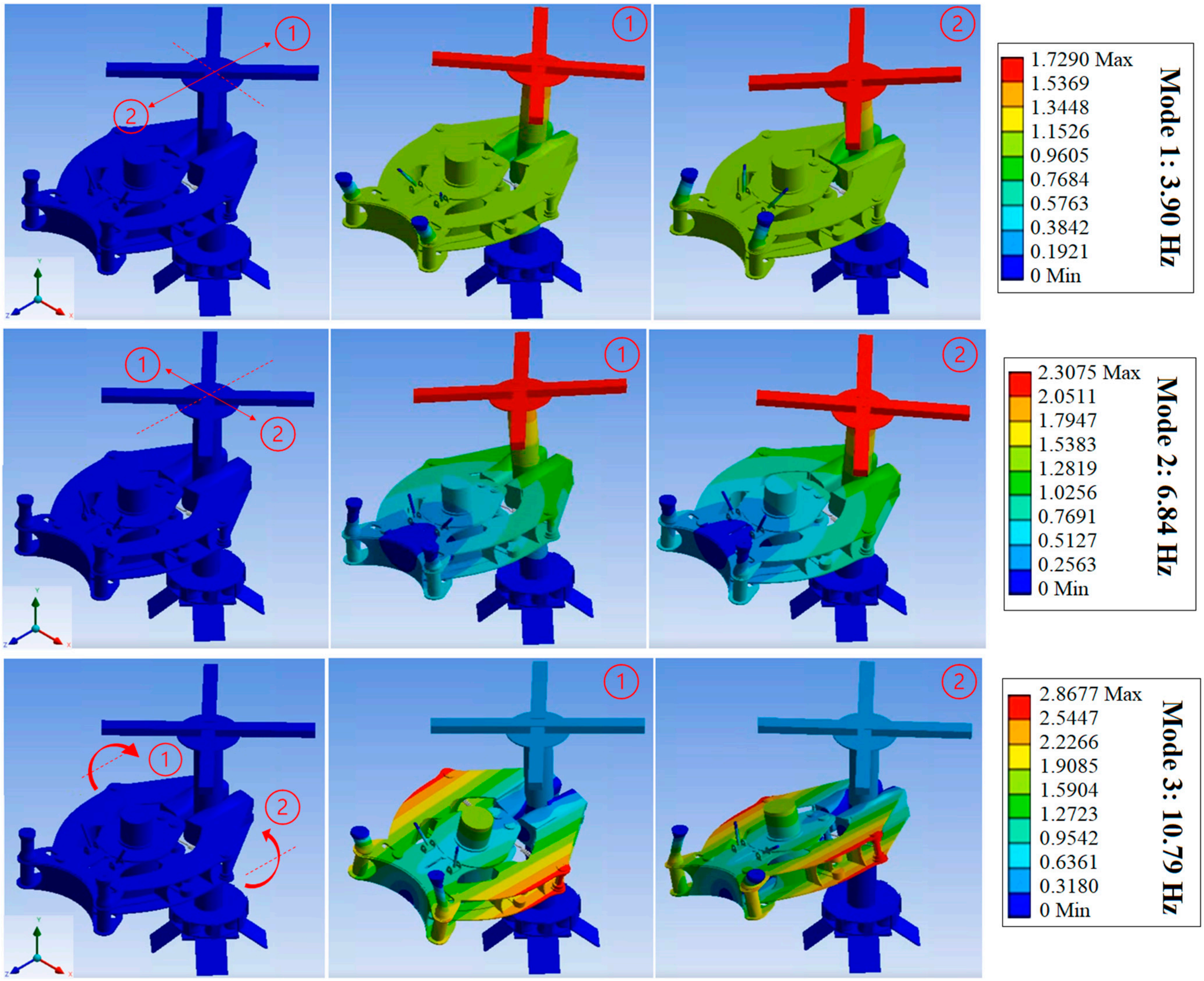

Figure 9. Deformations in mm calculated in the first 3 modes of the modal study. Positions 1 and 2 are the extremes in each mode.

5. Discussion

The points characterised in the acceleration recording work (Figure 3) provide information on the operation of the trunk shaker and have been commonly examined by various researchers [29,30]. However, to analyse the consistency of the computational model with respect to an experimental measurement, it is necessary to perform them on a test-bench such as the one used to obtain high repeatability (Figure 7) and to rule out uncertainties of other biomechanical variables. The point of application of the vibration is very important. Vibration propagation is facilitated by increasing the grip height of the trunk shaker leading to a reduction in driving force [21]. However, high gripping heights can provide excessive response in the branches and damage them. Conversely, setting the grip height close to the ground can cause root damage [31]. The diameter of the trunk to be gripped is also a factor to be considered in trunk shaker harvesting, since the larger the diameter, the higher the vibration power required to harvest the fruit [32]. Different studies have recorded the resulting acceleration generated in the trunk using trunk shakers with values of 60–170 m s^{-2} between 14–22 Hz for citrus [30] and 70–99 m s^{-2} between 22–26 Hz for olive trees [24]. These values are very similar to those measured in this work on the post in the grip, although with somewhat lower values on the test bench due to its higher stiffness. However, the values recorded on the test bench with one mass are practically identical to the accelerations measured on similar test benches: 54–94 m s^{-2} for frequencies 19 Hz [33].

The level of similarity between the simulations carried out with the experimental tests is very high when the machine is working free (Table 1). Nevertheless, greater deviations begin to be generated between the predicted accelerations when the machine-test bench binomial is simulated. Part of the differences observed in the frequency spectrum (Figure 6) between the experimental and simulated results are due to the distribution of the acceleration at different frequencies, which are not distributed in the same way. Experimental results revealed harmonics at higher frequencies, similar to those reported in other work on trunk shaker simulations [20].

It has been demonstrated that there is a relationship of increasing the resulting acceleration at any point with increasing frequency. However, as mentioned in the introduction section, each type of fruit tree has a range of frequencies determined to knock down the fruit efficiently, so that an increase in acceleration does not necessarily result in a higher percentage of fruit being knocked down. The study of the development of new trunk shakers must also incorporate the amplitude component needed in the tree trunk to obtain high harvesting efficiencies which is directly related to the mass and eccentricity of the rotating mass system of these machines [34].

On the contrary, increasing the mass to vibrate (test bench) has been shown to decrease the acceleration values recorded. This is related to the fact that for the same type of fruit tree, there may be differences in the efficiency of the same machine due to the diversity in tree morphology (mass, damping and stiffness) [10]. The amount of mass distributed in the tree, as well as the amount of leaves, fruit distribution or amount of wood in the tree structure directly affect the energy recorded for the same study point [8].

Harvesting fruit trees by trunk shaker requires adequate transmission of mechanical waves from the trunk to the branches, causing a movement in the fruit capable of overcoming the inertial force of the stalk and dropping it [21]. There is a loss of energy produced in the pads with the friction between the trunk shaker and the tree. This decrease is much more accentuated when the trunk shaker has been used in the test bench coinciding with other works carried out [20]. The transmissibility values measured in this work are quite like those reported from trunk-to-branch in different fruit trees and in computational models of trees [35]. Comparing the experimental vs. simulation results, a greater reduction in the transmitted acceleration is observed in the experimental tests than the simplifications carried out in the computational model in the simulation of the trunk shaker post-contact. This may be due to the modelling of the pads without considering their non-linear behaviour, to discrepancies in their real mechanical properties or to the type of simulated contact with the post. In particular, the type of contact established between solidary and fixed is known to be unrealistic due to the existing frictions. However, it is highly complicated to simulate the friction between the post and the pads and this would be a line of future work to improve the model. The simplifications made to the pads as a solid connection to the post reduce the computational load and enable the calculation to converge but introduce significant uncertainty in the results.

The displacements found along the test bench are caused by the unbalance produced by the eccentric mass of the trunk shaker. The modal analysis allows to detect possible failures in the shaker or in the test bench as well as the resonance effect. Other modal studies focus on the stem–fruit junction in order to know the stress/displacement required for dropping it [21]. The maximum deformations in the pads according to the simulations were found to be around 1 mm in Mode 2. High deformations in the post in the grip would lead to heats up in the pads and consequently to significant bark injuries in fruit trees. In this sense, the prediction of the acceleration orbits that the shaker can realise are also of vital importance. To ensure an adequate vibration distribution, the smaller value of the principal axes divided by the larger value of the principal axes should be equal to or greater than 0.5 [24].

6. Conclusions

The results obtained in experimental tests and computer simulations coincide precisely in the characterisation of the work of the trunk shaker free (error < 4%). The error in the resulting predicted accelerations is higher when the machine works attached to the post. The experimental vibration spectrum is very similar to that obtained with the simulations, although there is a different distribution of harmonics which may result in some differences in the resulting accelerations measured at the points of this work. In the cases of study, the error percentage is minimal in the trunk shaker, increase in the points of test bench, 1–20% for configuration with 23 Hz and 50–80% for configurations with 18 Hz. When the frequency of vibration is increased, the resulting accelerations increase in all cases; conversely, when the mass of the vibrating bench is increased, the resulting accelerations decrease. The vibration transmissibility is reduced between the trunk shaker and the post by 35–75% depending on the configuration studied but increases between the low post and the high post by 150–200%. The results of transmissibility and resultant values have a certain similarity with those measured in trees, although lower due to the stiffness of the system. The computational modal analysis revealed good results in the prediction of the generated acceleration orbits and the characterisation of the vibration modes of the assembly.

In summary, the proposed computational model offers an important potential in the development of these machines and their optimisation without the need of developing multiple pro-types and performing many field tests. However, in order to improve the results, future research should be directed towards improving the model in the type of contact generated between the pads and the tree or test post.

Author Contributions: Conceptualization, R.R.S.-G.; methodology, R.R.S.-G.; test, P.S.-C. and R.L.-M.; data collection, P.S.-C. and R.L.-M.; formal analysis, P.S.-C. and R.L.-M.; investigation, R.R.S.-G., Project administration and funding acquisition, R.R.S.-G.; writing, R.R.S.-G. and P.S.-C. All authors have read and agreed to the published version of the manuscript.

Funding: This work is part of the research Project "Optimisation of vibration technology for improving the efficiency of mechanised harvesting of fruit trees" (1381058-R) that has been co-financed by the Operational Programme FEDER 2014–2020 and by the Consejería de Economía, Conocimiento, Empresas y Universidad de la Junta de Andalucía.

Institutional Review Board Statement: Not applicable.

Informed Consent Statement: Not applicable.

Data Availability Statement: Not applicable.

Conflicts of Interest: The authors declare no conflict of interest.

References

1. Peterson, D.L.; Takeda, F. Feasibility of mechanically harvesting fresh market quality eastern thorneless blackberry. *Appl. Eng. Agric.* **2003**, *19*, 25–30. [CrossRef]
2. Pu, Y.; Toudeshki, A.; Ehsani, R.; Yang, F.; Abdulridha, J. Selection and experimental evaluation of shaking rods of canopy shaker to reduce tree damage for citrus mechanical harvesting. *Int. J. Agric. Biol. Eng.* **2018**, *11*, 48–54. [CrossRef]
3. Ravetti, L.; Robb, S. Continuous mechanical harvesting in modern Australian olive growing systems. *Adv. Hortic. Sci.* **2010**, *24*, 71–77.
4. Afsah-Hejri, L.; Homayouni, T.; Toudeshki, A.; Ehsani, R.; Ferguson, L.; Castro-García, S. Mechanical harvesting of selected temperate and tropical fruit and nut trees. *Hortic. Rev.* **2002**, *49*, 171–242.
5. Farinelli, D.; Ruffolo, M.; Boco, M.; Tombesi, A. Yield efficiency and mechanical harvesting with trunk shaker of some international olive cultivars. *Acta Hortic.* **2012**, *949*, 379–384. [CrossRef]
6. Affeldt, H.A.; Shackel, K.A.; Slaughter, D.C. Methodlogy for determining almond shaker dis-placement and frequency. *Trans. ASAE* **2003**, *19*, 141–144.
7. Brown, G.K.; Rauch, M.H.; Timm, E.J. Improved Clamp Pad for Trunk Shakers. *Trans. ASAE* **1988**, *31*, 677–682. [CrossRef]
8. Castro-Garcia, S.; Aragon-Rodriguez, F.; Arias-Calderón, R.; Sola-Guirado, R.R.; Gil-Ribes, J.A. The contribution of fruit and leaves to the dynamic response of secondary branches of orange trees. *Biosyst. Eng.* **2020**, *193*, 149–156. [CrossRef]
9. Spatz, H.C.; Theckes, B. Oscillation damping in trees. *Plant Sci.* **2013**, *207*, 66–71. [CrossRef]

10. Tombesi, S.; Poni, S.; Palliotti, A.; Farinelli, D. Mechanical vibration transmission and harvesting effectiveness is affected by the presence of branch suckers in olive trees. *Biosyst. Eng.* **2017**, *158*, 1–9. [CrossRef]
11. Whitney, J.D.; Smerage, G.H.; Block, W.A. Dynamic analysis of a trunk shaker-post system. *Trans. ASAE* **1990**, *33*, 1066–1070. [CrossRef]
12. Singiresu, S. *Vibraciones Mecánicas Quinta Edición*; Pearson Education: Mexico City, México, 2012.
13. Yung, C.; Fridley, R.B. Computer Simulation of Vibration of Whole Tree Systems Using Finite Element Methods. *Trans. ASAE* **1975**, *18*, 475–481. [CrossRef]
14. Ma, R.; Homayouni, T.; Toudeshki, A.; Ehsani, R.; Zhang, X. An Experimental Study and Mathematical Modeling of Vibration Transfer in Pistachio Trees Using an Inertia-Type Trunk Shaker and Field-Adapted Wireless Sensors. *Shock. Vib.* **2022**, *2022*, 111–125. [CrossRef]
15. Láng, Z. Dynamic modelling structure of a fruit tree for inertial shaker system design. *Biosyst. Eng.* **2006**, *93*, 35–44. [CrossRef]
16. El-Awady, M.N.; Genaidy, M.A.I.; Rashowan, M.; El- Attar, M.Z. Modeling and Simulating of Olive-Tree Harvesting Mechanism. *Misr J. Agric. Eng.* **2008**, *25*, 712–722. [CrossRef]
17. Bentaher, H.; Haddar, M.; Fakhfakh, T.; Mâalej, A. Finite elements modeling of olive tree mechanical harvesting using different shakers. *Trees-Struct. Funct.* **2013**, *27*, 1537–1545. [CrossRef]
18. Tang, X. Simulation of Vibration Harvesting Mechanism for Wolfberry. In *2011 Louisville, Kentucky, 7–10 August 2011*; American Society of Agricultural and Biological Engineers: St. Joseph, MI, USA, 2011.
19. Wu, C.; He, L.; Du, X.; Chen, S.; Ni, K. 3D reconstruction of Chinese hickory tree for dynamics analysis. *Biosyst. Eng.* **2014**, *119*, 69–79. [CrossRef]
20. Cetinkaya, C.; Polat, R.; Ozalp, A.F. Investigation of the vibration effect of using single or double eccentric mass in the trunk shakers used in fruit harvesting. *Eng. Sci. Technol. Int. J.* **2022**, *35*, 101228. [CrossRef]
21. Hoshyarmanesh, H.; Dastgerdi, H.R.; Ghodsi, M.; Khandan, R.; Zareinia, K. Numerical and experimental vibration analysis of olive tree for optimal mechanized harvesting efficiency and productivity. *Comput. Electron. Agric.* **2017**, *132*, 34–48. [CrossRef]
22. Wei, J.; Yang, G.Y.; Yan, H.; Jing, B.; Yu, Y. Rigid-flexible coupling simulation and experimental vibration analysis of pistachio tree for optimal mechanized harvesting efficiency. *Mech. Adv. Mater. Struct.* **2021**, *28*, 2360–2369. [CrossRef]
23. Niu, Z.; Xu, Z.; Deng, J.; Zhang, J.; Pan, S.; Mu, H. Optimal vibration parameters for olive harvesting from finite element analysis and vibration tests. *Biosyst. Eng.* **2022**, *215*, 228–238. [CrossRef]
24. Leone, A.; Romaniello, R.; Tamborrino, A.; Catalano, P.; Peri, G. Identification of vibration frequency, acceleration, and duration for efficient olive harvesting using a trunk shaker. *Trans. ASABE* **2015**, *58*, 19–26.
25. Abdel-Fattah, H.M.; Shackel, K.A.; Slaughter, D.C. Substantial vertical tree displacements occur during almond harvesting. *Am. Soc. Agric. Eng.* **2003**, *19*, 145–150.
26. Castro-García, S.; Gil-Ribes, J.A.; Blanco-Roldán, G.L.; Aguera-Vega, J. Mode shapes evaluation of trunk shakers used in oil olive harvesting. *Trans. ASABE* **2007**, *50*, 727–732. [CrossRef]
27. Patil, H.; Jeyakarthikeyan, P.V. Mesh convergence study and estimation of discretization error of hub in clutch disc with integration of ANSYS. In Proceedings of the 2nd International Conference on Advances in Mechanical Engineering (ICAME 2018), Kattankulathur, India, 22–24 March 2018; Volume 402.
28. Lalo, D.F.; Greco, M. Rubber bushing hyperelastic behavior based on shore hardness and uniaxial extension. In Proceedings of the 24th ABCM International Congress of Mechanical Engineering, COBEM-2017, Curitiba, Brazil, 3–8 December 2017; Volume 5280.
29. Recchia, L.; Boncinelli, P.; Sarri, D.; Rimediotti, M.; Vieri, M.; Cini, E.; Lisci, R. Recovery of waste biomass in nurseries. *Appl. Eng. Agric.* **2015**, *31*, 377–385.
30. Torregrosa, A.; Porras, I.; Martín, B. Mechanical harvesting of lemons (cv. Fino) in Spain using abscission agents. *Trans. ASABE* **2010**, *53*, 703–708. [CrossRef]
31. Sola-Guirado, R.R.; Bernardi, B.; Castro-García, S.; Blanco-Roldán, G.L.; Benalia, S.; Fazari, A.; Brescia, A.; Zimbalatti, G. Assessment of aerial and underground vibration trasmission in mechanically trunk shaken olive trees. *J. Agric. Eng.* **2018**, *788*, 191–197. [CrossRef]
32. Homayouni, T.; Gholami, A.; Toudeshki, A.; Afsah-Hejri, L.; Ehsani, R. Estimation of proper shaking parameters for pistachio trees based on their trunk size. *Biosyst. Eng.* **2022**, *216*, 121–131. [CrossRef]
33. Castillo-Ruiz, F.J.; Blanco-Roldán, G.L.; Jiménez-Jiménez, F.; Colmenero-Martinez, J.T.; Castro-Garcia, S.; Sola-Guirado, R.R.; Gil-Ribes, J.A. Comportamiento de un vibrador de troncos orbital sobre un poste de acero empotrado en zapata de hormigón. In Proceedings of the VIII Congreso Ibérico de Agroingeniería y Ciencias Hortícolas, Orihuela-Algorfa, Valencia, Spain, 1–3 June 2015.
34. López-Alba, E.; Dorado-Vicente, R.; Vasco-Olmo, J.; Díaz-Garrido, F.A. Diseño y desarrollo de una pinza vibradora para uso agrícola. *Dyna* **2012**, *87*, 114–119.
35. Peng, J.; Xie, H.; Feng, Y.; Fu, L.; Sun, S.; Cui, Y. Simulation study of vibratory harvesting of Chinese winter jujube (*Zizyphus jujuba* Mill. cv. Dongzao). *Comput. Electron. Agric.* **2017**, *143*, 57–65. [CrossRef]